Saudi Dental Journal (2022) **34**, 136–141

King Saud University

Saudi Dental Journal

www.ksu.edu.sa
www.sciencedirect.com

ORIGINAL ARTICLE

Effect of staining on the mechanical, surface and biological properties of lithium disilicate

Aline Serrado de Pinho Barcellos [a], Jean Soares Miranda [b], Marina Amaral [c], Janaína Araújo Alvarenga [d], Lafayette Nogueira [e], Estevão Tomomitsu Kimpara [e,*]

[a] *Post Graduation Program in Restorative Dentistry, Sao Paulo State University, Av. Eng. Francisco José Longo, 777 - Jardim Sao Dimas, São José dos Campos, SP 12245-000, Brazil*
[b] *Department of Dentistry, Federal University of Juiz de Fora (UFJF) - Campus Governador Valadares – Rua São Paulo, 745 – Centro, Governador Valadares, MG 35010-180, Brazil*
[c] *Department of Dentistry, University of Taubate, Rua dos Operários, 9, Taubate, SP, Brazil*
[d] *Department of Microbiology, Sao Paulo State University, Av. Eng. Francisco José Longo, 777 - Jardim Sao Dimas, São José dos Campos, SP 12245-000, Brazil*
[e] *Department of Dental Materials and Prosthesis, Sao Paulo State University, Av. Eng. Francisco José Longo, 777 - Jardim Sao Dimas, São José dos Campos, SP 12245-000, Brazil*

Received 7 August 2021; revised 8 December 2021; accepted 15 December 2021
Available online 20 December 2021

KEYWORDS

Glazing;
Physical properties;
Roughness;
Colony forming units

Abstract *Purpose:* To simulate biodegradation and wear of stained and glazed CAD lithium disilicate ceramic, and evaluate their effects on the microbial adherence and mechanical and surface properties of lithium disilicate ceramic

Materials and methods: 160 lithium disilicate ceramic discs were fabricated and divided in eight groups according to manual stain and glaze application with a fine paint brush (without stain and glaze; with stain and glaze) and aging procedures (no aging; wear at 30 N load, 1.7 Hz, 3×10^5 cycles; biodegradation by exposure to microcosm biofilm; biodegradation + wear; biodegradation + wear). Profilometry was performed to determine the surface roughness and the wear consequences. Biaxial flexural strength test was performed, and a *Streptococcus mutans* adherence test was conducted to evaluate the number of colony forming units.

Results: Unaged samples with and without stain and glaze presented the lowest values of surface roughness ($p < 0.001$), but after aging (wear, biodegradation, or both), the samples in the stain and glaze groups were rougher than those in the no stain and glaze groups ($p < 0.001$). The stain and glaze groups showed the highest volume of wear after aging ($p = 0.04$), and had the lowest flexural

* Corresponding author.
E-mail addresses: jeansoares@msn.com (J. Soares Miranda), janaina_2406@hotmail.com (J. Araújo Alvarenga), lafayette.nogueira-junior@unesp.br (L. Nogueira), estevao.kimpara@unesp.br (E. Tomomitsu Kimpara).
Peer review under responsibility of King Saud University.

Production and hosting by Elsevier

https://doi.org/10.1016/j.sdentj.2021.12.007

strength values ($p < 0.01$), irrespective of the aging method. The aging method did not affect the flexural strength ($p = 0.06$). The number of colonies forming units was higher for biodegradation + no stain and glaze, biodegradation + wear + no stain and glaze, no aging + stain and glaze, biodegradation + stain and glaze, and biodegradation + wear + stain and glaze. The lowest values were observed for no aging + no stain and glaze.

Conclusion: The staining and glazing of lithium disilicate increased the surface wear and bacterial adherence, and decreased biaxial flexural strength of the material. When exposed to S. mutans, surface roughness increased, and biodegradation favored bacterial adherence.

1. Introduction

Lithium disilicate (LD) ceramics are composed of a glass matrix and crystalline phase, and commercially presented as blocks for computer-aided design/computer-aided manufacturing (CAD/CAM) or injection ingots (Figueiredo-Pina et al., 2016). Both techniques result in monolithic restorations, which are usually finished with stains and glaze for the best esthetic result (Vidotti et al., 2013; Aurélio et al., 2015; Lin et al., 2012; Subaşı et al., 2014; Kanat-Ertürk, 2020).

Stains and glaze are fired after ceramic injection or crystallization, increasing the time of LD firing, and may result in alteration of mechanical properties (Miranda et al., 2020a), and may lead to an irregular and/or porous surface, which is prone to biofilm formation (Vo et al., 2015). The processing steps of LD may lead to stress concentration on the surface of LD (Subaşı et al., 2014), resulting in different surface characteristics (Aurélio et al., 2015; Abdalla et al., 2021; Fraga et al., 2015).

The interaction of ceramics with oral bacterial biofilm, salivary enzymes, and temperature and pH alterations may result on biofilm formation on ceramic surfaces and lead to chemical degradation of the material (Vo et al., 2015; Habib et al., 2020; Barcellos et al 2018). The degradation is caused by salivary enzymes and hydrolytic degradation, which break molecular linkages in the ceramic (Vo et al., 2015; Kermanshahi et al., 2010; Shokati et al., 2010), decreasing the strength, and accelerating bacterial infiltration and degradation of the material (Kermanshahi et al., 2010; Papadogiannis et al., 2011).

Chemical degradation, associated with vertical and oblique chewing loads, leads to ceramic surface degradation, decrease in strength and hardness, and increases the roughness of the ceramic surface (Papadogiannis et al., 2011), favoring biofilm formation (Kermanshahi et al., 2010; Papadogiannis et al., 2011; Hahnel et al., 2009). Thus, a ceramic degradation dynamic is formed: hydrolytic degradation + load application > rough surface > biofilm formation > bacterial penetration > increased chemical degradation > decrease in strength > fracture of ceramic.

The effect of bacteria on the clinical behavior of dental ceramics is relevant. The progression of biofilms on restorative materials may also be responsible for secondary caries at the ceramic-tooth interface, periodontal diseases or peri-implantitis (AAbdalla et al., 2021; Habib et al., 2020; Hahnel et al., 2009). The chemical degradation may also favor enhanced biofilm retention (Fúcio et al., 2008; Bourbia et al., 2013), and decrease the restorations longevity (Habib et al., 2020; Fúcio et al., 2008; Bourbia et al., 2013).

Thus, the aim of this study was to simulate biodegradation (exposure to biofilm) and wear of stained and glazed CAD/CAM LD ceramic, and evaluate their effects on the mechanical and surface properties, and microbial adherence to LD. The null hypothesis was that the aging procedure (no aging, wear, biodegradation, and wear associated with biodegradation) and staining and glazing would not affect LD properties.

2. Material and methods

2.1. Fabrication of samples

LD blocks (IPS e.max CAD, LTA3/ C14, Ivoclar Vivadent, Schaan, Liechtenstein) were cut into 12 mm diameter cylinders. They were sectioned (Extec High Concentration, Extec, Enfield, CT, EUA; Isomet 1000, Buehler, Plymouth, MN, EUA) into 160 discs (1.2 ± 0.2 mm thickness) (ISO 6872/2008). Discs were polished with silicon carbide paper (400 to 1200 grit, Norton, Guarulhos, SP, Brazil; Politriz, Buehler, Plymouth, MN, EUA) and cleaned in an ultrasonic bath.

The ceramic discs were subjected to one of the following procedures : no additional procedure (NO; n = 80), crystallization firing with a maximum temperature of 850 °C for 28 min (Programat EP 3000, Ivoclar Vivadent), as recommended by the manufacturer; and stain and glaze (SG; n = 80), crystallization firing as mentioned above, followed by staining (IPS e.max Ceram Shades, Ivoclar Vivadent, Schaan, Liechtenstein) and glazing (IPS e.max Ceram Glaze Liquid, Ivoclar Vivadent, Schaan, Liechtenstein). Firing of the stain and glaze was performed in a single cycle, with a maximum temperature of 770 °C for 17 min (Miranda et al., 2020a).

2.2. Aging procedures

Four aging procedures were performed (n = 20 each): control (**ctrl**) – no aging; surface wear (**we**) with a spherical stainless steel load applicator tip (Ø 3.5 mm), positioned in the center of the sample, and slid 6 mm horizontally (30 N load, 1.7 Hz, 3×10^5 cycles) with samples immersed in distilled water at 25 °C (Biocylce V2, Biopdi, São Carlos, SP, Brazil) (Subaşı et al., 2014); biodegradation (**bi**) with exposure of samples to a biofilm formed by the microcosm method with mucin (Montagner et al., 2016); and biodegradation followed by surface wear (**bw**). The groups formed were NO-ctrl, NO-we, NO-bi, NO-bw, SG-ctrl, SG-we, SG-bi, and SG-bw.

The microcosm method was used. The present study was approved by the local research ethics committee (protocol # 2.819.810). Biofilms were formed on the ceramic samples in 24-well microtiter plates (KASVI, Curitiba, Brazil) and the saliva of two volunteers was used to produce the microcosm. Volunteers did not present active carious lesions, had good general health, and had not used antibiotics in the previous 12 months. Each volunteer donated 20 mL of saliva for immediate use. In each well of the plate, 0.4 mL of fresh saliva, 1.8 mL of brain heart infusion solution (BHI, Himedia, Mumbai, India) and 0.5% sucrose were inoculated on the ceramic discs.

The plates with the ceramic discs and microcosms were placed in a bacteriological incubator under agitation (37 °C, 5 Hz, 7 days). Each sample was gently washed by immersion in 2 mL sterile 85% sodium hypochlorite solution for 10 s, removing the non-adherent bacteria. Samples were placed in new plates with microcosm and BHI solution, and again placed in the bacteriological incubator (Rudney et al., 2012). The microcosm and BHI solution were renewed every 7 days for a period of 30 days for biodegradation. The samples were then exposed to ultraviolet radiation for decontamination.

2.3. Profilometry

Surface roughness was measured (n = 15) using a digital optical profilometer (Wyko, Model NT 1100, Veeco, Tucson, EUA) and an image software (Vision 32, Veeco, EUA). One measurement (Ra value) was performed at the center of each sample from a distance of 1.6 mm with a velocity of 0.05 mm/s. Data were subjected to parametric one-way analysis of variance (ANOVA) and Tukey's test ($\alpha = 0.05$).

The amount of material removed by wear was also measured by profilometry in the NO-ctrl, NO-we, NO-bw, SG-ctrl, SG-we, and SG-bw groups (n = 10). Profilometry (CyberSCAN CT 100, Cyber TECHNOLOGIES GmbH, Eching-Dietersheim, Alemanha) was performed using a profile and 3D software analysis (SCAN 8.6.5546, Cyber TECHNOLOGIES, Germany), with 3000 mm × 2000 ms, to obtain a 3D image that allowed the measurement of the surface wear. Data obtained were compared using Kruskal-Wallis inferential analysis.

2.4. Biaxial flexural strength test

The biaxial flexural strength test (n = 15) was performed (EMIC DL-1000, EMIC, Sao Jose dos Pinhais, Brazil) according to ISO 6872/2008 (piston-on-three-ball design). Data were subjected to parametric ANOVA and Tukey's post hoc test ($\alpha = 0.05$).

2.5. Microbial adherence (CFU counting)

Ceramic samples (n = 5) were sterilized in an autoclave at 121 °C for 20 min. The reference strain S. mutans UA 159 was used. The S. mutans strain was grown in brain heart infusion (BHI) broth (HiMedia, Mumbai, India) supplemented with 5% sucrose (Sigma-Aldrich, St. Louis, MO, USA), at 37 °C and 5% CO2 for 24 h (Vilela et al., 2012). After growth, the culture was centrifuged and the pellet was washed twice with 0.85% NaCl. The standardized suspensions were adjusted using a Micronal B582 spectrophotometer (Microtek Laboratories, São Paulo, Brazil) to 10^6 cells/mL.

S. mutans biofilm was formed on ceramic samples (n = 5), according to Vilela et al., 2012. The sterilized discs were positioned in the wells of 24-well culture plates (Corning, Corning, NY, USA), then a 250-μL aliquot of the standard suspension of S. mutans (10^6 cells/mL) was added on the surface of each LD sample containing 1.75 mL BHI broth supplemented with 5% sucrose. The culture was incubated for 4 h (5% CO_2, 37 °C). Discs were washed 3 times with 0.85% NaCl, and the S. mutans biofilms were detached using a Sonopuls HD 2200 ultrasonic homogenizer (Bandelin Electronic, Berlin, Germany) at 50 W for 30 s. The suspensions were serially diluted and plated on BHI agar to determine the CFU/mL. The numerical values of CFU obtained for the samples were subjected to the parametric ANOVA, and Tukey's post hoc test ($\alpha = 0.05$).

2.6. Scanning electron microscopy (SEM)

Representative samples of each group were etched with hydrofluoric acid (5%, 60 s), and their surfaces were observed under a scanning electron microscope (MIRA 3, Kohoutovice, Czech Republic). For the microbial adherence test analysis, samples were subjected to overnight fixation with 2.5% glutaraldehyde solution and dehydrated with ethanol (70%–85%–95% and twice with absolute ethanol, 30 min each) prior to sputter coating with gold-palladium alloy.

3. Results

3.1. Profilometry

The mean surface roughness (Ra) was affected by the aging method ($p < 0.001$), staining and glazing ($p < 0.00$), and by the interaction of factors ($p < 0.001$). NO-**ctrl** and SG-**ctrl** presented the lowest values of Ra, but after aging (**we**, **bi**, or **bw**), the samples in the SG (SG-**we,** SG-**bi,** SG-**ctrl** and SG-**bw)** groups were rougher than those correspondent in the NO groups (NO-**we,** NO-**bi,** NO-**ctrl** and NO-**bw)** (Table 1).

Regarding volumetric profilometry results (Table 1 and Fig. 1), aging (**we** or **bw**), and staining and glazing (SG) affected the volume of wear ($p = 0.04$): the SG groups (SG-**we** and SG-**bw)** presented higher volume of wear after aging than the NO groups (NO-**we** and NO-**bw)**.

3.2. Biaxial flexural strength test

The highest flexural strength was observed in the NO-**ctrl** group (Table 1), similar to NO-**bi** and NO-**bw** ($p < 0.01$). The lowest flexural strength values were observed in the SG groups (SG-ctrl, SG-**we,** SG-**bi,** SG-**ctrl** and SG-**bw)**, despite the aging method. Aging did not affect the flexural strength ($p = 0.06$).

3.3. Microbial adherence (CFU)

Aging **(we, bi or bw)** affected the number of CFUs in the NO groups ($p < 0.01$) (Table 1), but staining and glazing (SG) did not ($p = 0.84$). The interaction between these factors was sig-

Table 1 Ra (μm), wear by volumetric profilometry (μm^3), biaxial flexural strength (MPa) and CFU (CFU/ml[log10]) from the tested groups, with respective standard deviation (SD) and significance.

Group	Ra (SD)	Volume wear (SD)	Biaxial flexural strength (MPa)	CFU (SD)
NO-**ctrl**	0.05 (0.02) ^{d}	–	284.40 (57.0) ^{a}	7.66 (0.09) ^{d}
NO-**we**	1.62 (0.25) ^{c}	92 (0.8) ^{b}	218.60 (50.2) ^{bc}	7.85 (0.04) ^{bc}
NO-**bi**	0.31 (0.08) ^{d}	–	236.06 (33.1) ^{abc}	7.97 (0.06) ^{ab}
NO-**bw**	2.08 (0.27) ^{b}	81 (0.2) ^{b}	241.10 (71.5) ^{ab}	8.00 (0.04) ^{a}
SG-**ctrl**	0.13 (0.04) ^{d}	–	161.30 (52.4) ^{d}	7.95 (0.04) ^{ab}
SG-**we**	2.15 (0.76) ^{b}	188 (0.9) ^{a}	158.40 (54.7) ^{d}	7.80 (0.07) ^{c}
SG-**bi**	1.88 (0.25) ^{bc}	–	184.68 (33.0) ^{cd}	7.89 (0.03) ^{abc}
SG-**bw**	2.98 (0.06) ^{a}	145 (0.7) ^{a}	194.72 (31.3) ^{cd}	7.87 (0.02) ^{abc}

Different superscript letters indicate statistical difference in the same column.

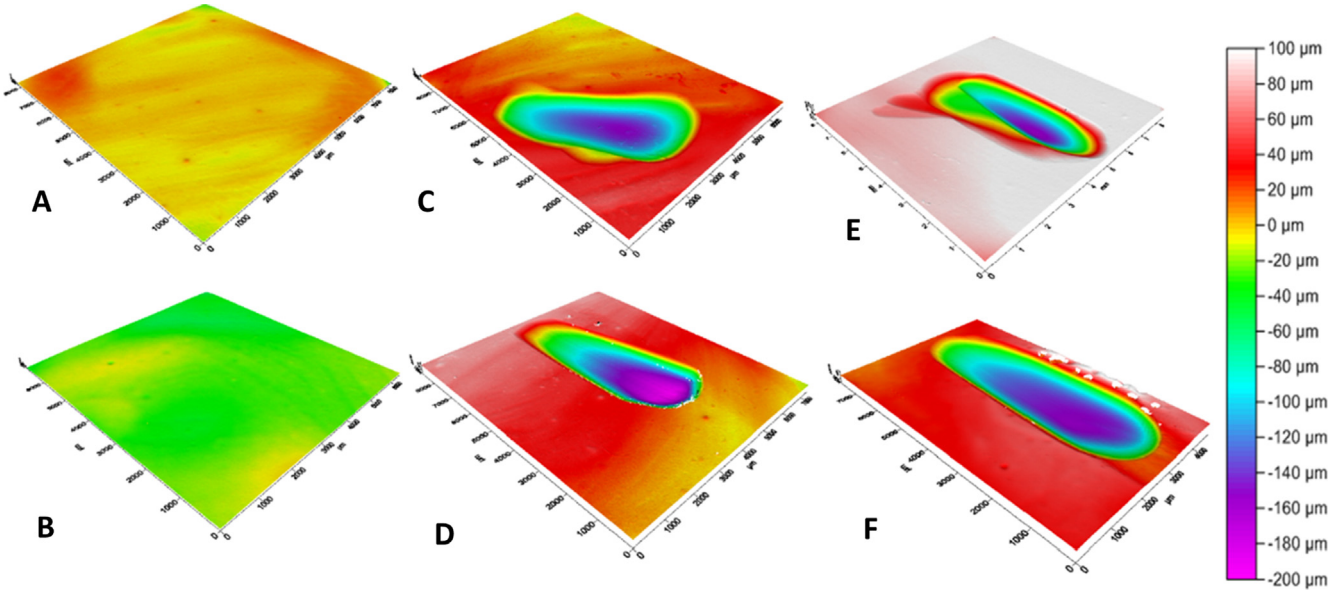

Fig. 1 3D profilometry of the surfaces of the samples after wear: A) NO-ctrl; B) SG-ctrl; C) NO-we; D) SG-we; E) NO-bw; F) SG-bw.

nificant ($p < 0.01$). The number of CFU was the highest in the NO-**bi**, NO-**bw**, SG-**ctrl**, SG-**bi**, and SG-**bw** groups (Table 1).

3.4. SEM analyses

SEM images (Fig. 2) showed different surface patterns among the groups. On SG-**we** samples, stain and glaze were removed after the wear test, exposing the LD surface. On SG-**bw** samples, scratches were observed on the LD surface, with some residual stain and glaze. Samples from the WO-**bi** and SG-bi groups presented spots of bacterial colonization, and those from the SG-bi group showed surface porous. On samples exposed to biofilm (**bi and bw**), it was possible to observe the growth of microorganisms and the formation of an extracellular matrix (Fig. 2).

4. Discussion

Staining and glazing were associated with biodegradation and wear, and led to the highest values of surface roughness (SG-**bw**). Such procedures also resulted in the highest surface wear of the material (SG groups) and the lowest biaxial flexural strength (SG groups). Samples exposed to biodegradation associated with or without wear (NO-**bi**, NO-**bw**) and with staining and glazing (SG-**ctrl**, SG-**bi**, SG-**bw**) presented the highest number of CFUs.

The literature lacks of information about the effects of biofilms and their products on the surface properties of dental materials. Ceramic, without any intervention (aging or coloring), is a smooth and inert material (Al Moaleem et al, 2020; Montazerian and Zanotto, 2017), which does not interact with the oral environment, not stimulatin the formation of biofilm. Al Moaleem et al. (2020) showed that Streptococcus adhere poorly to ceramic surface. Some studies report that the roughness and adherence of *S. mutans* could be related (Abdalla et al., 2021; Habib et al., 2020), but others do not agree (Papadogiannis et al., 2011). According to our results, the null hypothesis was not accepted. The control groups NO and SG presented similar and the lowest roughness values, but after aging, the SG groups presented the highest Ra values, showing the effect of staining and glazing on roughness. The effect of biodegradation on roughness was noticed as the Ra values of NO-**ctrl** and SG-**ctrl** were similar, but NO-**bi** presented lower

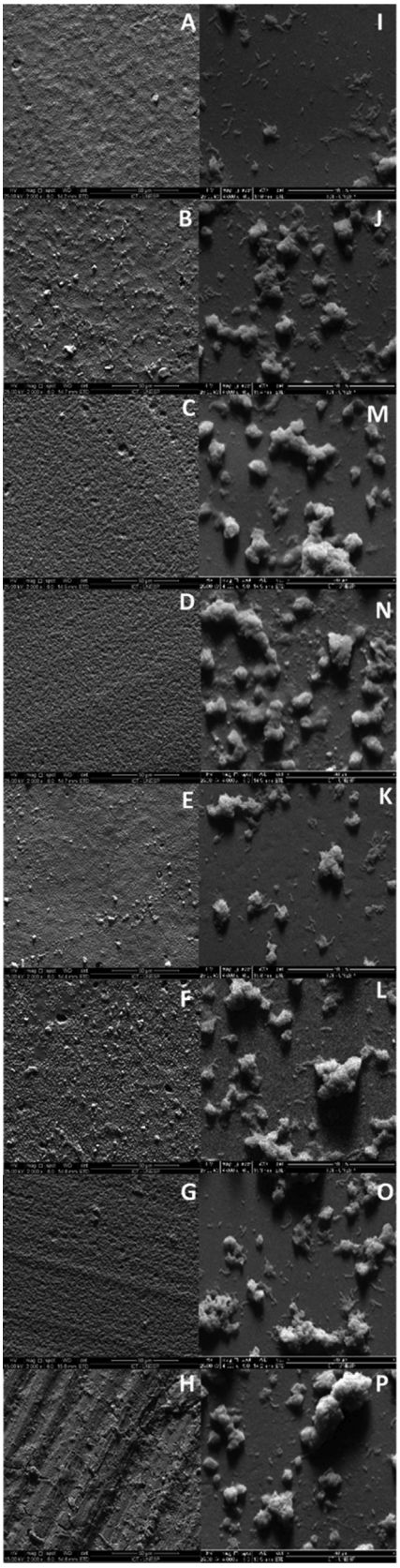

Fig. 2 Surface micrographs of samples that were not exposed to biodegradation (A: NO-ctrl; B: SG-ctrl; C: NO-we; D: SG-we; E: NO-bi; F: SG-bi; G: NO-bw; H: SG-bw) (2000×), and those that were (I: NO-ctrl; J: SG-ctrl; K: NO-we; L: SG-we; M: NO-bi; N: SG-bi; O: NO-bw; P: SG-bw) (4000×).

Ra values than SG-**bi**. Such effect could be explained by both the amount and size of crystals in the stain/glaze and in the LD ceramic (Vo et al., 2015; Miranda et al., 2020b), and the fabrication method; while NO samples were produced by machining, SG samples received additional hand application of stain and glaze, which may have resulted in an irregular and porous surface with macroscopic defects (Vo et al., 2015; Miranda et al., 2020b; De Jager et al., 2000; Sun et al., 2016; Hmaidouch et al., 2014).

Regarding the volumetric profilometry analysis (Table 1), the SG groups presented the highest wearc. Fig. 1 shows similar images for NO-**ctrl** and SG-**ctrl**, but significant values of material loss are shown in Table 1. Besides the wear of LD shown by the NO groups, the SG groups presented wear of the stain/glaze layer (Sun et al., 2016; Hmaidouch et al., 2014). The stain and glaze materials have low strength, and are composed mainly of a glassy matrix; thus, they were completely worn during wear (Lin et al., 2012; Miranda et al., 2020a; Belli et al., 2014; Zhang et al., 2016; Sabrah et al., 2013; Bai et al., 2016).

Staining and glazing decreased the biaxial flexural strength (Table 1). In the NO groups, the aging promoted by wear also decreased the flexural strength. Because the stain/glaze layer was positioned down during the biaxial flexural strength, strength values were affected by this layer (Lin et al., 2012; Belli et al., 2014; Zhang et al., 2016; Miranda et al., 2020a; Borba et al., 2011). In addition to the amorphous structure, the hand application of stain and glaze is also prone to voids, which favor fracture at lower stress values (Miranda et al., 2020a). Wear decreased the strength of the samples in the NO groups compared to other aging methods, probably due to the creation of harmful defects such as microcracks, leading to a decrease in strength (Lin et al., 2012; Belli et al., 2014; Zhang et al., 2016; Rashid, 2014).

The null hypothesis that microbial adherence would not be affected by staining and glazing and aging procedures was not accepted, since the lowest values of CFU were presented by NO-**ctrl**. After aging or stain/glaze application, there was an increase in the number of CFU (Table 1). No-**ctrl** and SG-**ctrl** presented the lowest values of surface roughness, but surface roughness may not be directly related to microbial adherence (Hahnel et al., 2009). Biofilm formation involves more complex processes, such as the presence of different microorganisms in a biofilm and receptor-linking recognition, (Vo et al., 2015; Wessel et al., 2014). Groups that underwent biodegradation (NO-**bi**, NO-**bw**, SG-**bi**, and SG-**bw**) presented the highest number of CFUs, probably due to the previous contact with the biofilm during biodegradation. However, SG-**ctrl** presented the highest values of CFU, probably caused by *S. mutans* adherence and growth in surface voids. No additional procedures for LD ceramic (NO-**ctrl**) presented the best results for roughness, wear, strength, and microbial adherence. Contact with the biofilm (NO-**bi**) resulted in an increase in CFU.

The present study has limitations, as it was an in vitro study that employed only a single microorganism, *S mutans*, while true biofilms in vivo are much more heterogeneous. In addition, this study did not quantify the adhesion forces of microbial cells to the ceramic surface. Wear and biofilm exposure are an inevitable reality in oral rehabilitation, but when esthetics are not critical (posterior regions), surface polishing of LD ceramic restorations should be preferred over stain/glaze application.

5. Conclusions

Staining and glazing of lithium disilicate ceramic surfaces increase the surface wear and bacterial adherence, while decrease the biaxial flexural strength of the material. When associated with exposure to S. mutans biofilm, the surface roughness increased. Moreover, biodegradation itself favors bacterial adherence.

Declaration of Competing Interest

The authors declare that they have no known competing financial interests or personal relationships that could have appeared to influence the work reported in this paper.

References

Abdalla, M.M., Ali, I.A.A., Khan, K., Mattheos, N., Murbay, S., Matinlinna, J.P., Neelakantan, P., 2021. The influence of surface roughening and polishing on microbial biofilm development on different ceramic materials. J. Prosthodont. 30 (5), 447–453.

Al Moaleem, M.M., Porwal, A., Al Ahmari, N.M., Shariff, M., 2020. Oral biofilm on dental materials among Khat Chewers. Curr. Pharm. Biotechnol. 21 (10), 964–972.

Aurélio, I.L., Fraga, S., Dorneles, L.S., Bottino, M.A., May, L.G., 2015. Extended glaze firing improves flexural strength of a glass ceramic. Dent. Mater. 31, 316–324. https://doi.org/10.1016/j.dental.2015.10.012.

Bai, Y., Zhao, J., Si, W., Wang, X., 2016. Two-body wear performance of dental colored zirconia after different surface treatments. J. Prosthet. Dent. 116, 584–590.

Barcellos, A.S.P., Marinho, C.C., Miranda, J.S., Amaral, M., Shiino, M.Y., Kimpara, E.T., 2018. Effect of fatigue protocols on flexural strength of lithium disilicate bars with clamped-ends. J. Mech. Behav. Biomed. Mater. 81, 173–177.

Belli, R., Geinzer, E., Muschweck, A., Petschelt, A., Lohbauer, U., 2014. Mechanical fatigue degradation of ceramics versus resin composites for dental restorations. Dent. Mater. 30, 424–432.

Borba, M., de Araújo, M.D., de Lima, E., Yoshimura, H.N., Cesar, P. F., Griggs, J.A., Della Bona, A., 2011. Flexural strength and failure modes oflayered ceramic structures. Dent. Mater. 27, 1259–1266.

Bourbia, M., Ma, D., Cvitkovitch, D.G., Santerre, J.P., Finer, Y., 2013. Cariogenic bacteriad egrade dental resin composites and adhesives. J. Dent. Res. 92, 989–994.

De Jager, N., Feilzer, A.J., Davidson, C.L., 2000. The influence of surface roughness on porcelain strength. Dent. Mater. 16, 381–388.

Figueiredo-Pina, C.G., Patas, N., Canhoto, J., Cláudio, R., Olhero, S. M., Serro, A.P., Ferro, A.C., Guedes, M., 2016. Tribological behaviour of unveneered and veneered lithium disilicate dental material. J. Mech. Behav. Biomed. Mater. 53, 226–238.

Fraga, S., Valandro, L.F., Bottino, M.A., May, L.G., 2015. Hard machining, glaze firing and hydrofluoric acid etching: Do these procedures affect the flexural strength of a leucite glass-ceramic? Dental Mater.: Off. Publ. Acad. Dental Mater. 31, e131–e140.

Fúcio, S.B., Carvalho, F.G., Sobrinho, L.C., Sinhoreti, M.A., Puppin-Rontani, R.M., 2008. The influence of 30-day-old Streptococcus mutans biofilm on the surface of esthetic restorative materials–an in vitro study. J. Dent. 36, 833–839.

Habib, S.R., Nakshabandi, A.Z., Al Shawi, A.A., Allohaidan, F.A., Al Kurdi, R.B., AlSarhan, M., 2020. Degree of Streptococcus mutans colonization on common restorative materials subjected to wear cycle. Int. J. Prosthodont. 10.11607/ijp.6519.

Hahnel, S., Rosentritt, M., Handel, G., Bürgers, R., 2009. Surface characterization of dental ceramics and initial streptococcal adhesion in vitro. Dent. Mater. Off. Publ. Acad. Dental Mater. 25, 969–975.

Hmaidouch, R., Müller, W.D., Lauer, H.C., Weigl, P., 2014. Surface roughness of zirconia for full-contour crowns after clinically simulated grinding and polishing. Int. J. Oral Sci. 6, 241–246.

Lin, W.S., Ercoli, C., Feng, C., Morton, D., 2012. The effect of core material, veneering porcelain, and fabrication technique on the biaxial flexural strength and weibull analysis of selected dental ceramics. J. Prosthodontics 21, 353–362.

Kanat-Ertürk, B., 2020. Color stability of CAD/CAM ceramics prepared with different surface finishing procedures. J. Prosthodontics 29, 166–172.

Kermanshahi, S., Santerre, J.P., Cvitkovitch, D.G., Finer, Y., 2010. Biodegradation of resin-dentin interfaces increases bacterial microleakage. J. Dent. Res. 89, 996–1001.

Miranda, J.S., Barcellos, A., Campos, T., Cesar, P.F., Amaral, M., Kimpara, E.T., 2020a. Effect of repeated firings and staining on the mechanical behavior and composition of lithium disilicate. Dent. Mater. 36, e149–e157.

Miranda, J.S., Barcellos, A., MartinelliLobo, C.M., Caneppele, T., Amaral, M., Kimpara, E.T., 2020b. Effect of staining and repeated firing on the surface and optical properties of lithium disilicate. J. Esthetic Restorative Dentistry 32, 113–118.

Montagner, A.F., Maske, T.T., Opdam, N.J., de Soet, J.J., Cenci, M. S., Huysmans, M.C., 2016. Failed bonded interfaces submitted to microcosm biofilm caries development. J. Dent. 52, 63–69.

Montazerian, M., Zanotto, E.D., 2017. Bioactive and inert dental glass-ceramics. J. Biomed. Mater. Res. A 105 (2), 619–639.

Papadogiannis, D., Tolidis, K., Lakes, R., Papadogiannis, Y., 2011. Viscoelastic properties of low-shrinking composite resins compared to packable composite resins. Dent. Mater. J. 30, 350–357.

Rashid, H., 2014. The effect of surface roughness on ceramics used in dentistry: a review of literature. Eur. J. Dent. 8, 571–579.

Rudney, J.D., Chen, R., Lenton, P., Li, J., Li, Y., Jones, R.S., Reilly, C., Fok, A.S., Aparicio, C., 2012. A reproducible oral microcosm biofilm model for testing dental materials. J. Appl. Microbiol. 113, 1540–1553.

Sabrah, A.H., Cook, N.B., Luangruangrong, P., Hara, A.T., Bottino, M.C., 2013. Full-contour Y-TZP ceramic surface roughness effect on synthetic hydroxyapatite wear. Dent. Mater. 29, 666–673.

Shokati, B., Tam, L.E., Santerre, J.P., Finer, Y., 2010. Effect of salivary esterase on the integrity and fracture toughness of the dentin-resin interface. J. Biomed. Mater. Res. Part B, Appl. Biomater. 94, 230–237.

Subaşı, M.G., Demir, N., Kara, Ö., Ozturk, A.N., Özel, F., 2014. Mechanical properties of zirconia after different surface treatments and repeated firings. J. Adv. Prosthodontics 6, 462–467.

Sun, S., Liang, R., Ren, J., Xu, Y., Zhao, Y., Meng, H., 2016. Influence of polishing and glazing on the wear of zirconia and enamel. Chinese J. Stomatol. 51, 300–304.

Vidotti, H.A., Garcia, R.P., Conti, P.C., Pereira, J.R., Valle, A.L., 2013. Influence of low concentration acid treatment on lithium disilicate core/veneer ceramic bond strength. J. Clin. Exp. Dent. 5, e157–e162.

Vilela, S.F., Junqueira, J.C., Barbosa, J.O., Majewski, M., Munin, E., Jorge, A.O., 2012. Photodynamic inactivation of Staphylococcus aureus and Escherichia coli biofilms by malachite green and phenothiazine dyes: an in vitro study. Arch. Oral Biol. 57, 704–710.

Vo, D.T., Arola, D., Romberg, E., Driscoll, C.F., Jabra-Rizk, M.A., Masri, R., 2015. Adherence of Streptococcus mutans on lithium disilicate porcelain specimens. J. Prosthetic Dentistry 114, 696–701.

Wessel, S.W., Chen, Y., Maitra, A., van den Heuvel, E.R., Slomp, A. M., Busscher, H.J., van der Mei, H.C., 2014. Adhesion forces and composition of planktonic and adhering oral microbiomes. J. Dent. Res. 93, 84–88.

Zhang, Y., Mai, Z., Barani, A., Bush, M., Lawn, B., 2016. Fracture-resistant monolithic dental crowns. Dental Mater. 32, 442–449.